Biol. Cybern. 76, 207–215 (1997)

Biological Cybernetics


# On Hebbian-like adaptation in heart muscle: a proposal for 'cardiac memory'

**Srinivasa V. Chakravarthy**[1], **Joydeep Ghosh**[2]

[1] Division of Neurosience, Baylor College of Medicine, Houston, TX 77030, USA
[2] Department of Electrical and Computing Engineering, The University of Texas, Austin, TX 78712, USA

Received: 26 October 1995 / Accepted in revised form: 23 October 1996

**Abstract.** Studies on the effects of external pacing of heart suggest that the organ, like the nervous system, possesses the properties of 'memory' and adaptation. Changes induced in cardiac activation patterns persist long after the agent that induced those changes itself is removed. After the effects of stimulation have disappeared, response to the stimulus applied for a second time is much greater than the earlier response. Motivated by such results, this paper further explores the possibility of a 'cardiac memory'. In particular, we point out that communication via gap junctions in cardiac tissue is similar to synaptic conductance in nervous tissue and demonstrate, with the aid of a mathematical model, that cardiac tissue can exhibit memory-like behavior if gap-junctional conductances are allowed to adapt according to a Hebbian-like mechanism.

## 1 Introduction

It is well known that the mammalian heart is an electromechanical organ, driven by a local conduction system, with higher regulatory influence coming from the central nervous system. Although the cardiac conduction system functions as a local nervous system, conduction is not via neurons, but by special excitable muscle cells known as the 'myocardiac' cells, or simply cardiac cells. An intriguing study of external ventricular activation of the mammalian heart, conducted by Rosenbaum et al. (1982) has shown that effects of activation include 'the properties of "accumulation" and "memory", that is, the change in the duration of the excited state takes a certain time to become apparent, a very long time to reach its maximal effect . . . and occurs in a much shorter time when the heart has been previously *conditioned* (italics our) by the same perturbation.' Analogies between 'heart memory' and the processes of learning and retrieval which occur in the brain were subsequently made (Rosenbaum et al. 1985).

In the present study, we approach the phenomenon of cardiac memory from the connectionist perspective. Several connectionist models of neural memory and learning are based on a cellular mechanism known as Hebbian learning (Hebb 1949). Comparing the physiology of cardiac and neural tissues, we point out a possible cellular basis for cardiac memory effect. We hypothesize that conductances of intercellular channels in cardiac tissue adapt in an activity-dependent manner according to some form of Hebbian mechanism. A model of cardiac electrical activity that incorporates this mechanism is constructed. The model is not meant to be a detailed cellular-level representation of the heart but, rather, emphasizes three features of heart function: (1) synchronized oscillations, (2) out-of-phase activity of atrial and ventricular regions, and (3) persistent effects of external stimulation, or the cardiac memory effect.

The paper is outlined as follows. In Sect. 2, basic cardiac physiology and electrical activity are briefly reviewed. Evidence pointing to activity-dependent adaptation in cardiac tissue is presented and past models of cardiac oscillations are reviewed. In Sect. 3, a new model is proposed to explain some of the salient aspects of normal heart function. The model is used to describe synchronized oscillations in the heart and development of normal atrioventricular (AV) rhythms, in Sect. 4. In Sect. 5, clinical evidence for cardiac memory is detailed and a simple situation is simulated using the model. In the final section, the present work is placed in perspective with relevant facts from physiology.

## 2 Cardiac physiology and modeling

### *2.1 Synchronous oscillations in heart function*

Cardiac cells are *autorhythmic*, i.e., they produce action potentials (AP) spontaneously. This forms the basis of the heart's semi-autonomous function. Cardiac cells are connected by cell-to-cell junctions called *gap junctions* (GJ) (Loewenstein 1981), which permit conduction of APs from one cell to another. In this respect, GJs are similar to synaptic junctions. However, synaptic transmission is chemical, whereas GJ conduction is by direct movement of ions. Moreover, GJ conduction is bidirectional, as opposed to unidirectional transmission across the synapse. GJs permit large areas of cardiac tissue to contract as a single unit, a functional

*Correspondence to*: J. Ghosh (e-mail: ghosh@ece.utexas.edu)

*syncytium*, by synchronizing the oscillations of a large number of cells. Synchronized cellular oscillations are found to play an important role in the visual cortex also (Gray and Singer 1989).

### *2.2 Evidence for gap junction adaptation*

Electron microscopic images of cell-to-cell contact regions of early chick heart suggest involvement of GJs in coupling of embryonic heart cells (De Mello 1982). When pairs of embryonic heart cells are brought into contact in a culture medium, they begin to beat in synchrony and GJs appear at about the same time. In cultured heart cells, the time required for GJ junction formation and synchronization varies from a few minutes to an hour (De Haan and Hirakow 1972). At the time of cell contact the coupling conductance is quite low, but increases to a high value once synchronization is complete (Clapham et al. 1980).

The GJ conductance does not depend on transjunctional potential; but it depends on the potential across nonjunctional membrane (Obaid and Rose 1981). In one instance, GJ conductance between a pair of cells fell on both depolarization and hyperpolarization of either cell, although in an asymmetric fashion (Smith and Baumann 1969). In another case, conductance fell only on depolarization (of nonjunctional membrane) (Socolar and Politoff 1971). Although no formal mechanism relating individual cell potentials and GJ variation has ever been proposed, studies on the role of coupling resistance on synchronization exist (Jalife et al. 1988). Using pacemaker cells from rabbits, Jalife et al. observed that when two cells are connected through low-resistance links, the period of resulting phase-locked firing is a function of their respective intrinsic frequencies, their phase relationship, and the connecting resistance. The evidence presented above seems highly suggestive of a mechanism of GJ formation involving individual activities of the connected cell pair.

### *2.3 Pacemaking and cardiac rhythms*

Each cardiac cell on the heart's surface has a characteristic oscillation frequency, which decreases as one goes from the top (base) towards the bottom (apex) of the heart. In classic textbook accounts (Guyton 1981), a group of pacemaker cells, which beat at the fastest rate, are described as setting the pace of the heart. If different cells beat at different frequencies how can faster cells 'set the pace' for slower ones? And how can the entire heart beat at a single frequency? The problem arises due to a manner of describing in physiologically intuitive terms, phenomena that are appropriately or more accurately described using terms of electrical circuits and dynamical systems.

Experiments with cultured embryonic (Clapham et al. 1980) and adult (Jalife et al. 1988) cardiac tissues have shown that the firing frequency of a group of synchronous pacemaking cells is not the same as the intrinsic frequency of the fastest cell. De Haan and coworkers have demonstrated that when two groups of cells oscillating at different frequencies are brought into close contact, all the cells synchronize to a common frequency (Veenstra and De Haan 1988). These studies reveal that isolated cells beat at different 'intrinsic frequencies' in a tissue culture. Inside a normally functioning human heart they phase-lock and beat at a common frequency of about 72 beats per minute.

The heart, then, is a network comprised mostly of oscillating cells; some cells exhibit electrical oscillations only and primarily play the role of rhythm generation and conduction [the sino-atrial (SA) nodal cells and Purkinje fibers for instance]; in others electrical oscillations cause mechanical contractions (the muscle cells of atria and ventricles), and these take part in the pumping action of the heart. Proper cardiac function requires appropriate phase relations among cellular oscillations. These phase relations may vary smoothly, as a way of adapting to changing load situations, or dramatically, leading to random activation patterns known as the cardiac arrhythmias.

### *2.4 Nonlinear models of cardiac cell oscillations*

The first analog nonlinear model describing cardiac conduction was proposed by van der Pol and von der Mark (1928). The oscillator model they used is motivated by a biological neuron model, namely the Fitzhugh-Nagumo (FN) neuron (Fitzhugh 1961; Nagumo et al. 1962), which is derived by simplifying the Hodgkin-Huxley (HH) model for the squid neuron (Hodgkin and Huxley 1952). Even though the HH model is based on the squid neuron the principles are found to be applicable to a wide range of excitable cells. It was even found that with slight modifications the HH model can be manipulated to produce plateau-shaped cardiac APs also (Noble 1979). The FN model was also used to describe scroll waves in a sheet of excitable model cells (Panfilov and Winfree 1985); experimental evidence for such scroll waves in fibrillating cardiac tissue exists (Medvinsky et al. 1984).

An electrical analog of three oscillators, the so-called van der Pol oscillators (corresponding to the SA node, atria and ventricles), was studied by van der Pol and var der Mark (1928). The waveforms recorded from the network resembled the atrial and ventricular signals of the electrocardiogram. Subsequently, systems of a small number of van der Pol oscillators have been used to describe dynamics of cardiac cells (Guevera and Glass 1982) and to characterize pathological situations (Goldberger et al. 1985). However, in all these models there is no activity-dependent adaptation of coupling strengths. A network of FN model oscillators was proposed as a neural associative memory by Abbot (1990). A distinctive feature of this model is that the FN system is solved in a semirigorous form, and conditions for phase-locking derived. The coupling strengths between oscillators do not adapt, but can be precalculated so that desired patterns are stored in the network.

From the preceding discussion two things are clear: (a) the FN model exhibits oscillations under certain conditions, and a network of FN cells can be used to describe cardiac rhythms; (b) the same model can also be used as an associative memory by setting the coupling strengths appropriately. The possibility of constructing a biologically plausible 'cardiac memory' is already in the offing.

## 3 The model

The proposed model is a network of cells with complex-valued states that adapts using a Hebbian mechanism and has the properties of an associative memory. A detailed description and the mathematical properties of the model are presented elsewhere (Chakravarthy and Ghosh 1995). In this paper we describe its salient features and show how it models some aspects of cardiac activity. The equations of dynamics of a network of cells can be expressed as

$$\dot{z_j} = \sum_k T_{jk} V_k - (\nu + i(1-\nu)) z_j + I_j \tag{1}$$

$$V_j = g(\lambda(\nu + i(1-\nu)) z_j^*) \tag{2}$$

where the cell state, denoted by $z$, is a complex number, $I_j$ is the sum of the external currents entering the $j$th cell, Re[·] denotes the real part of the argument, and '*' denotes complex conjugate. The quantity Re[$V$] denotes the transmembrane cell potential. $T_{jk}$, a complex quantity, is the GJ conductance connecting $j$th and $k$th cells. The function $g(\cdot)$ is a complex function and taken to be equal to the tanh(·) function in the simulations.

The model exists in two distinct modes. (i) the fixed-point or dissipative mode, and (ii) the oscillatory or conservative mode. Mode switching can be done by varying a *mode parameter* ($\nu$). The above model is similar to the van der Pol (1926) model in that the latter also exhibits both fixed-point and oscillatory behavior (Abbot 1990). However, the equations describing the two models differ widely.

### *3.1 Fixed-point mode ($\nu$ = 1)*

The network operates in fixed-point mode when the mode parameter $\nu$ = 1, and the dynamics are given by:

$$\frac{dz_j}{dt} = \sum_k T_{jk} V_k - z_j + I_j \tag{3}$$

$$V_j = g(z_j^*) \tag{4}$$

If the conductance matrix, $T$, is a Hermitian, the dynamics are stable since a Lyapunov function, $E$, can be associated with the above system (Chakravarthy and Ghosh 1995). Hence the above equations of dynamics describe a *dissipative* system. $V$ usually settles in a fixed point, with each Re[$V_j$] approaching $\pm 1$. When Re[$V_j$] = 1, the $j$th cell is said to be 'depolarized', and when Re[$V_j$] = $-1$ it is 'repolarized' or simply polarized.

An activity-dependent adaptation mechanism for GJ conductances is given as:

$$\dot{T}_{jk} = -T_{jk} + g(z_j^*) g(z_k) \tag{5}$$

A significant consequence of the above adaptation procedure (5) is that when an external input, $I$, is presented to the network for a sufficiently long time, $T$ is modified such that the network 'memorizes' the input. Similar schemes have been proposed in the past to describe 'synaptic adaptation' in connectionist models of neuronal memories (Cohen and Grossberg 1983; Kosko 1988).

### *3.2 Oscillatory mode ($\nu$ = 0)*

The network exhibits oscillatory behavior when $\nu$ is set to 0 in (1, 2). In this case, the output of each neuron does not tend smoothly to $\pm 1$ as in the fixed point case, but flips between +1 and $-1$, producing a square-like waveform. The equations of dynamics (1, 2) are now expressed as

$$\dot{z_j} = \sum_k T_{jk} V_k - i z_j + I_j \tag{6}$$

$$V_j = g(i\lambda z_j^*) \tag{7}$$

The dynamics in this mode are fundamentally different from the fixed-point mode, since (6, 7) describe a *conservative system* (Chakravarthy and Ghosh 1995).

Similar to the fixed-point case, GJ adaptation in oscillatory mode is given as

$$\dot{T}_{jk} = -T_{jk} + g(i z_j^*) g(i z_k) \tag{8}$$

where, $g(\cdot) \equiv \tanh(\lambda \cdot)$. In this case, it is not straightforward to derive a Lyapunov function since for fixed $T$, (6) is a conservative system. But numerical simulations show that the system (6, 8) exhibits a remarkable stability, just like its dissipative counterpart. This might be due to the decay term ($-T_{jk}$) in (8). Also, if the activation dynamics (6) are frozen and only the GJ conductances are allowed to adapt, it is easy to see that a Lyapunov function can be associated with (8).

In this mode, the effect of external input is to modify and determine phase relations among oscillatory outputs of individual cells. The performance of the system can be best illustrated using a simple example.

*Example 1.* Consider a two-neuron network with the conductance matrix $T$ randomly initialized such that $T_{jk} \in [0, 1]$ for $j, k = 1, 2$. A constant input vector, $I = \{1, -1\}$, is presented to the network for 300 time steps and (6, 8) are simulated. The input, $I$, is then removed ($I$ = 0) and the simulation is continued. The cell outputs Re[$V_1$] and Re[$V_2$] are plotted against time in Fig. 1a. Variation in $T_{12}$ and $T_{21}$ is shown in Fig. 1b. Initially the phase difference between cell outputs is arbitrary. However, when the input is presented, conductances begin to adjust in such a way that external input is encoded in the form of phase difference between cell outputs. Since the inputs to cells are +1 and $-1$, the corresponding output waveforms must be exactly out of phase. After 300 time steps, when the input is removed, phase difference has not yet reached the desired value. A value of 180° is approached subsequently as conductances continue to adapt even after the input is removed.

We have seen that in the oscillatory mode the network tries to remember an external input in the form of phase relations among oscillations of individual cells.

### *3.3 Intermediate scenario*

So far we have presented two widely differing scenarios of the model. But neither of these models alone can describe the situation in cardiac tissue. Cardiac cells from different regions in the heart have different frequencies (Barry 1942), and therefore a model in which all the cells have the same

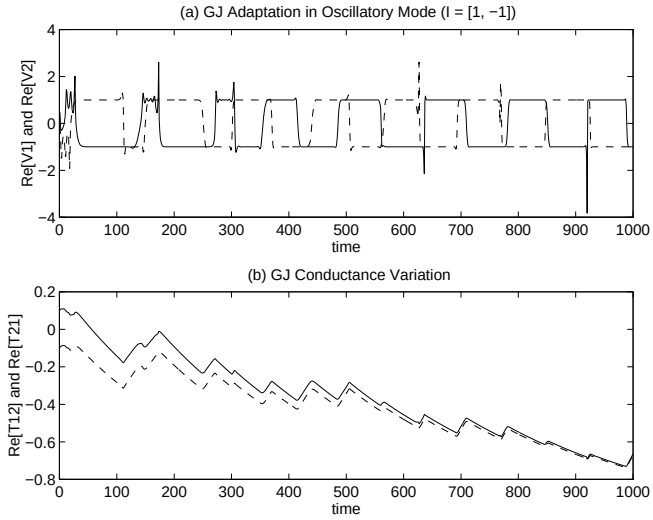


**Fig. 1a,b.** Gap junctional (GJ) adaptation in the oscillatory mode ($\nu = 0.0$). Input is removed after 300 time steps. **a** *continuous line,* Re[$V_1$]; *broken line,* Re[$V_2$]. **b** *continuous line,* Re[$T_{12}$]; *broken line,* Re[$T_{21}$]

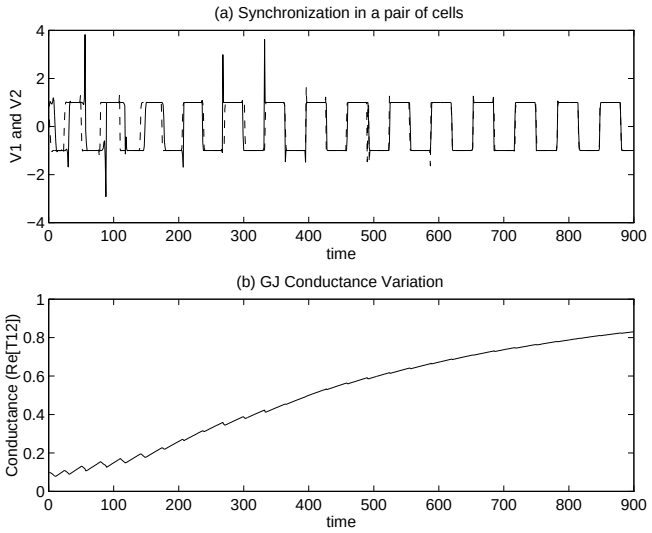


**Fig. 2a,b.** Coupling between a pair of cells oscillating at the same frequency ($\nu = 0.1$). **a** Cell outputs (*continuous line,* cell 1; *broken line,* cell 2 **b** Conductance $T_{12}$

frequency is inadequate. Also not all cardiac cells are oscillatory since the AV nodal cells are usually considered to be nonoscillating (De Mello 1977), driven by oscillatory inputs.[1] Therefore a network consisting only of oscillating cells is also an inappropriate representation. Consequently, we require a model with a more composite behavior.

Taking a closer look at the equations (1, 2), one may note that the mode parameter, $\nu$, which has so far been used to describe global behavior, is actually a local parameter in individual cells. A wider range of dynamic behavior is obtained by allowing $\nu$ to vary from cell to cell. For the case of a single cell, as $\nu$ is varied gradually from 0 to 1, oscillation frequency initially increases slightly but soon starts decreasing until at a critical value of $\nu$ it drops to 0, indicating a transition from the oscillatory to the fixed-point mode (Chakravarthy and Ghosh 1995).

However, for the network in a generic mode no such simple characterization is possible. For instance, even in a network with the same $\nu$ in all the cells, the point of mode transition depends on conductance values also. The two modes are simply described to give an idea of the extremes between which the generic mode lies. These may help a better understanding of the context-specific models that will be encountered in the following sections and in which the following general equations will be used:

$$\dot{z_j} = \sum_k T_{jk} V_k - (\nu + i(1-\nu)) z_j + I_j \tag{9}$$

$$V_j = g(\lambda(\nu + i(1-\nu)) z_j^*) \tag{10}$$

$$\dot{T}_{jk} = -T_{jk} + V_j V_k^* \tag{11}$$

[1] Actually, AV nodal rhythmicity is a much debated point (Guntheroth et al. 1983). The issue is deferred to the final section. For more details refer to Chakravarthy and Ghosh (1995).

## 4 Gap junction formation and rhythm development

In this section, we will show that the proposed mechanism for GJ adaptation accounts for synchronization of APs. Using qualitative information from physiology, a simple 'whole-heart' model is constructed. Using the model we will demonstrate that out-of-phase AV rhythms, which are indispensable for normal heart function, emerge naturally as a result of GJ adaptation.

We will consider a simple case of coupling between a pair of cells oscillating at the same frequency ($\nu_1 = \nu_2 = 0.1$). Equations (9–11) are used for simulation. The conductance matrix, $T$, is initialized as: $T_{11} = T_{22} = 1.0$, and $T_{12} = T_{21} = 0.1$. No external input is present. Conductance (Re[$T_{12}$] or Re[$T_{21}$]) is plotted in Fig. 2b. It can be seen that as conductance approaches a maximum, phase difference between the cell outputs goes to zero (Fig. 2). In a complementary situation, if the initial phase difference were negative, the two cells are eventually exactly out of phase, and conductance approaches a negative maximum.

### *4.1 Out-of-phase atrioventricular activity*

The following experiments are intended to demonstrate that (i) the characteristic top-to-bottom frequency gradient in the heart and (ii) Hebbian adaptation of GJ conductances, are responsible for the emergence and maintenance of the required phase difference between the atrial and ventricular regions. Since this is only a preliminary study, we will restrict ourselves to a simple model, which will be expanded in the future.

The model consists of a rectangular array of cells, a schematic of which is shown in Fig. 3. The array is divided into three areas of different average intrinsic frequencies: the region at the top (A) with the highest intrinsic frequency – the atrial region; the thin strip in the middle consisting of non-oscillating cells – the AV region; and the area at the

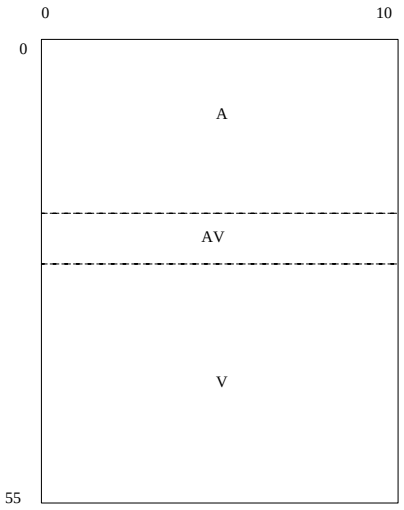


**Fig. 3.** The 'whole-heart' model. *A*, atrial region; *V*, ventricular region; *AV*, atrioventricular region

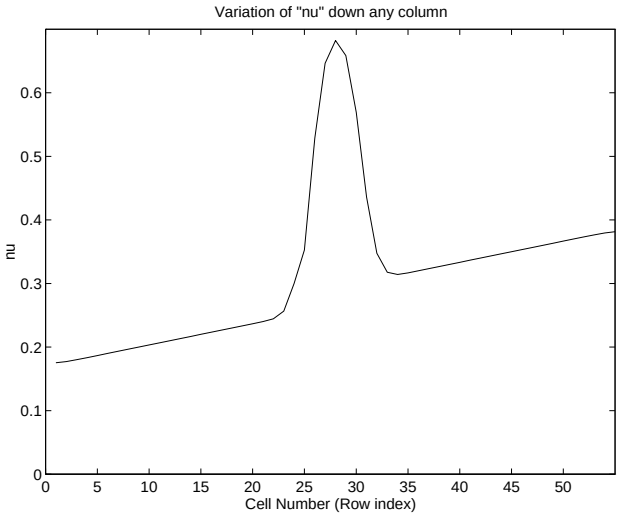


**Fig. 4.** Variation of $\nu$, down a column in the 'whole-heart' model shown in Fig. 3.

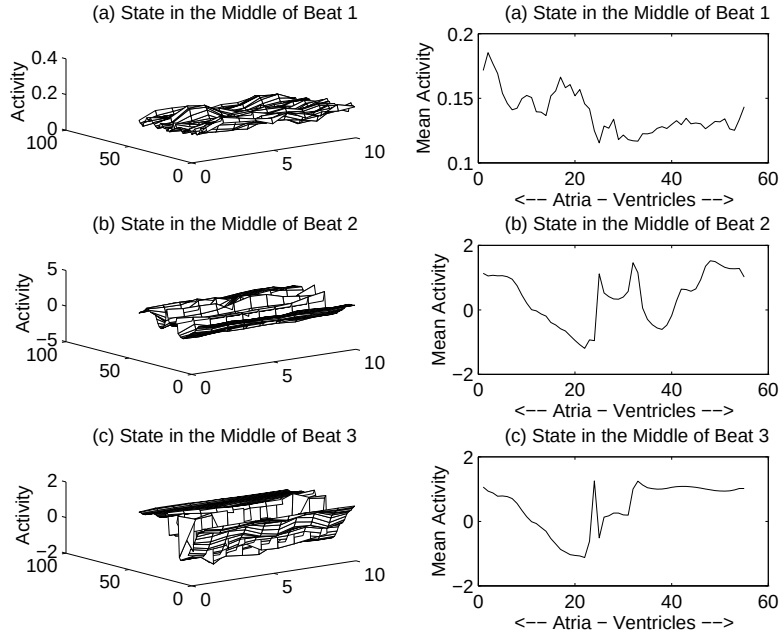


**Fig. 5a–c.** Development of atrioventricular rhythms: GJ adaptation is present during beats 1, 2 and 3

bottom (V) with a lower frequency – the ventricular region. For a detailed justification for the above 'lumped' model see Chakravarthy and Ghosh (1995).

### *4.2 Simulation*

An array, $H_{jk}$, of $55 \times 10$ cells (Fig. 3) is chosen for simulations. Intrinsic frequency decreases (i.e., $\nu$ increases) down the columns, except in the AV region. There is no variation along rows. Length-wise variation of $\nu$ is shown in Fig. 4. Though there are no rigid demarcations between different regions, rows $1 - -26$ can be related to atria, $27 - -30$ to the AV node, and the remaining rows to the ventricles. No left-right asymmetry of heart chambers is incorporated.

The neighborhood of each cell consists of: two successive 'northern' neighbors ($n1$ and $n2$), two 'southern' neighbors ($s1$ and $s2$), and one each of 'eastern' ($e1$) and 'western' ($w1$) neighbors. Cell dynamics and adaptation are governed by the following equations:

$$\begin{aligned} u_{j,k}(t+1) = u_{j,k}(t) + \eta_1(&w_0 H_{j,k}(t) + w_{n1} H_{j,k-1}(t) \\ &+ w_{n2} H_{j,k-2}(t) + w_{s1} H_{j,k+1}(t) + w_{s2} H_{j,k+2}(t) \\ &+ w_{e1} H_{j+1,k}(t) + w_{w1} H_{j-1,k}(t) \\ &- (\nu_{j,k} + i(1-\nu_{j,k}))u_{j,k}(t)) \\ H_{j,k}(t) = tanh(&\lambda(\nu_{j,k} + i(1-\nu_{j,k}))u^*_{j,k}(t)) \\ w_{ab}(t+1) = w_{ab}(t) + \eta_2(&-w_{ab}(t) + H_a(t)\beta H^*_b(t)) \end{aligned}$$

where $w_{ab}$ is the GJ conductance between cells $a$ and $b$ in $H$, if the two cells are connected. Numerical values of some of the main parameters are as follows: $\lambda$ = 1.5, $\beta$ = 0.25, $\eta_1$ = 0.08, $\eta_2$ = 0.007. The relative time-scales $\eta_1$ and $\eta_2$ in the above equations are artificial and are only meant to

reflect the fact that the time-scale of activation dynamics is much higher than that of GJ adaptation. All the 'mutual conductances' ($w_{s1}$, etc.) are initialized to a small value (= 0.1), whereas all the 'self-conductances' ($w_0$) are initialized to 0.6. With the above settings it is found that the average beat period is about 60 time steps. Only an average value can be given because the state $H$ is not strictly periodic in time even after the rhythms have fully matured.

Snapshots of $H$ at various stages of simulation are shown in Figs. 5a–c, 6a–c, and 7a–c. Each subplot of the figures depicts the state of $H$ at a single instant. Surface plots of Re[$H$] are shown in the left halves. The quantity Re[$H$] is a voltage, but no units are indicated in the plots because the values shown need not be faithful to physiology. For clarity, breadth-wise averaged activity, a sort of a 'side-view' of the surface plot, is depicted in graphs on the right-hand side, since not much breadth-wise variability is expected.

In the middle of beat 1, when adaptation has not proceeded far enough, activity is still low everywhere. In the right half of Fig. 5a one may note relatively higher activity in the atria, indicating that atria begin to depolarize before ventricles. Figure 5b describes the situation in the middle of beat 2. Half the atrial region is fully depolarized, while the half closer to the AV region is in the process of depolarizing. Another depolarizing wave has started from the outer end of the ventricular area. This is quite contrary, however, to the normal activation sequence in the heart. But we must remember that adaptation has not yet matured enough to produce a meaningful activation sequence. In beat 3 (Fig. 5c) atrial depolarization has not progressed much, but the ventricles are fully depolarized although in the wrong sequence. At the end of the third beat, adaptation is stopped and conductances are not varied any more. This division of the course of simulation into adapting and nonadapting stages is only to emphasize the role of adaptation in rhythm development.

The subsequent fourth beat, divided into six phases, is depicted in Figs. 6 and 7. In Fig. 6a, the atria are almost completely repolarized but for a small area adjacent to the AV region. The ventricles also are almost fully repolarized but a small swelling depolarizing wave can be noticed nearer to the AV region. In Fig. 6b, atrial repolarization is about 90% complete and a large depolarizing wave is spreading down the ventricles. Atrial repolarization has commenced in Fig. 6c, and proceeded nearly half-way into the atria. Ventricular depolarization is almost complete. Note that a large phase difference between atrial and ventricular activation patterns has already appeared.

In Fig. 7a, atrial depolarization is more that 50% complete and ventricles are fully depolarized. In Fig. 7b, atrial depolarization is complete and a repolarizing wave has begun spreading over the ventricles starting from the AV region. In Fig. 7c, atrial repolarization commenced and ventricular repolarization has progressed more that 50%.

The process continues in subsequent beats with a considerable delay between atrial and ventricular activations. The propagating impulse may be regarded as a traveling wave whose direction of propagation depends on the local frequency gradient. The impulse seems to originate from a point of locally maximal intrinsic frequency and spread to neighboring areas. Physiologically, such regions are described as 'pacemaking zones'. Two such zones are located in the model: (i) one at the top of region A, and (ii) another near the junction between AV and V regions. However, it must be noted that the point of origination does not exactly coincide with the point where the intrinsic frequency is locally maximum, but only close to it.

The two pacemaking zones mentioned above functionally correspond to the SA node and the AV node. Note that the functional 'AV node' is located near the junction of AV and V regions and not in the AV region itself. This might be the reason why the controversy over AV nodal rhythms is sometimes resolved by replacing the term 'nodal rhythms' with 'junctional rhythms' (Guntheroth et al. 1983). Thus a pacemaking zone appears to be a functional entity and not a clearly distinguishable anatomical unit. Such a view demands a revision of the classical notion of pacemaking zones.

Note that in the model repolarization and depolarization proceed in the same direction, both in the atria and in the ventricles. This is contrary to the situation in the human heart. However, by extensive simulations we have found that the order of repolarization critically depends on the distribution of $\nu$ chosen. For a slightly modified distribution of $\nu$ we have obtained a sequence in which repolarization and depolarization occur in the opposite direction, both in the atria and in the ventricles. Of course, this too is not physiologically appropriate. More realistic behavior might probably be achieved if a quantitatively accurate distribution of $\nu$ is chosen.

An interesting development occurs with regard to the conductance values, as a result of adaptation. Conductances of GJs connecting north-south neighbors ($w_{s1}, w_{s2}, w_{n1}$ and $w_{n2}$) are mostly positive in the A and V regions but negative in the AV region. The remaining (east-west) conductances are, however, generally positive everywhere. It is not clear what negative conductances mean in physiological terms. But as far as dynamics are concerned, it only means that the oscillating A and V regions are coupled by an inhibitory connection. This seems to cause the observed phase difference between atrial and ventricular activations.

## 5 Cardiac memory

### *5.1 Clinical findings*

Memory-like effects in the heart were observed by Rosenbaum and associates (1982) in connection with T-wave abnormalities in the human electrocardiogram. The T-wave corresponds to repolarization of ventricles. Classically, two types of abnormalities, primary and secondary, are recognized (Wilson et al. 1931). The secondary T-wave changes, which occur and disappear instantaneously, are triggered by changes in activation sequence, as occurring, for instance, in a left bundle branch block. The primary type, which are more persistent, are supposed to be due to a change in ventricular intrinsic frequency gradient.

In Rosenbaum et al. (1982), T-wave inversion was produced by atrial pacing, indirectly inducing a left bundle branch block. In this case, the inversion progressed gradually during pacing and plateaued after prolonged pacing. Inversion persisted for much longer period of time, even after

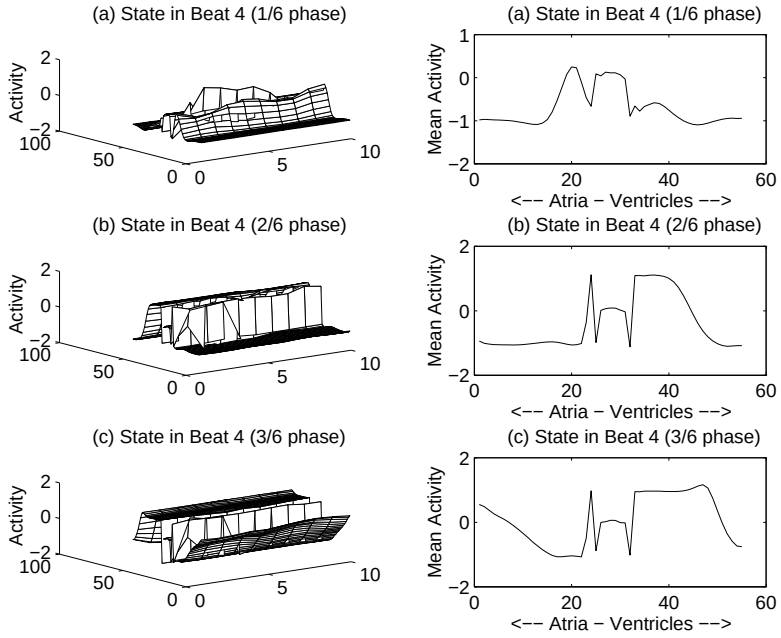


**Fig. 6a–c.** Development of atrioventricular rhythms: No GJ adaptation

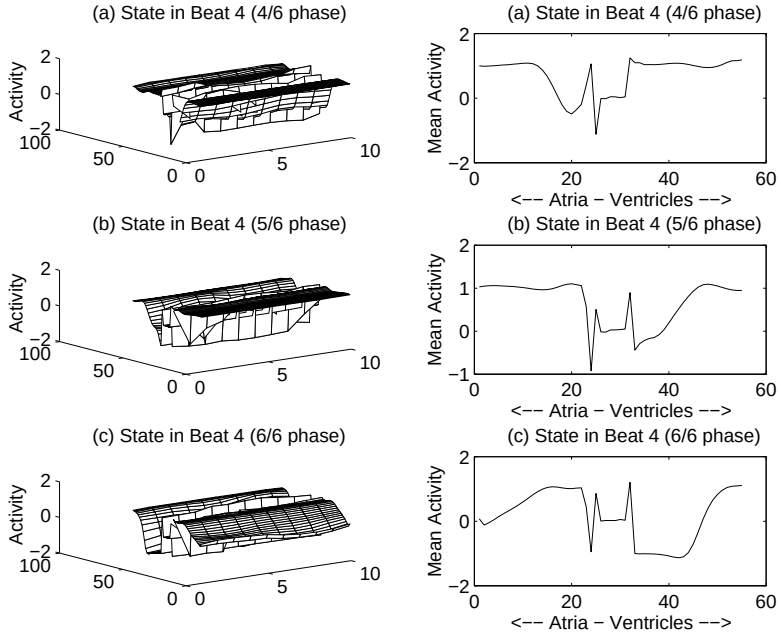


**Fig. 7a–c.** Development of atrioventricular rhythms: no GJ adaptation

pacing was discontinued, and left bundle branch block was no longer present, showing the property of ‘accumulation’. In another experiment, the authors used a discontinuous pacing sequence, with 15 min of pacing periods separated by non-pacing intervals in which the changes returned to normal, and observed that each successive pacing trial produced a greater degree of change than the previous one. These results suggest that the cells involved in the process seem to keep a ‘memory’ of the previous effect.

Such effects were attributed to electrotonic interactions operating during the course of activation (Toyoshima and Burgess 1978). When an activation sequence lasts sufficiently long it modulates electrotonically the existing order of ventricular activation. Rosenbaum et al. (1982) suggest that such modulation might be a ‘general law of the cardiac muscle’, underlying the observed effects of accumulation and memory: ‘Electrotonic modulation “teaches” the cells to repolarize in a particular order, and the longer the teaching lasts, the better the cells “learn” their lesson . . . The mechanism of this fascinating electrophysiological behavior is unknown . . . ’

We will now demonstrate that the physiological mechanism mentioned above is none other than GJ adaptation. When a particular activation sequence is induced for prolonged periods, the gap junctions are ‘modulated’ in such a way that the sequence persists for a while. We will now construct a simple model in which external stimulation at the center of an array of cells induces an ‘ectopic’ pacemaker even though no frequency gradient exists near the center.

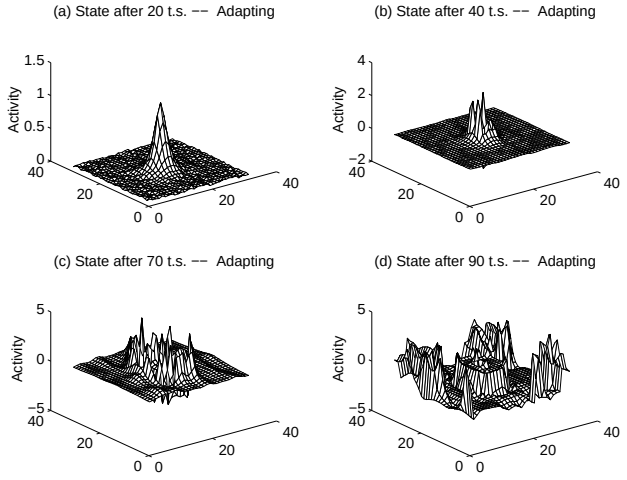


**Fig. 8a–d.** Induced activation sequence in an array of cells with uniform intrinsic frequency distribution. Sequence is induced by an oscillatory stimulus applied maximally at the center of the array, tapering towards the edges. *t.s.,* time steps

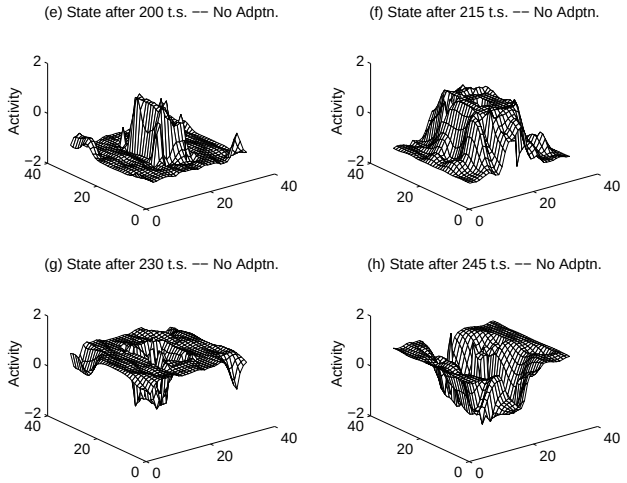


**Fig. 9e–h.** Persistence of the activation sequence induced in Fig. 8. No stimulus is present and conductances are not adapted (*No Adptn.*). *t.s.,* time steps

### *5.2 Simulation*

To model cardiac memory, we chose an array $M$, of size $32 \times 32$, consisting of oscillating cells ($\nu$ = 0.2 in all cells). Hence, there is no preferred location for impulse origination, nor a select direction for its propagation. The whole array is locally driven by an oscillatory input of period 64 time steps. The stimulating signal is generated by another oscillating cell with $\nu$ = 0.1 (other parameters are fixed as: $\lambda$ = 1.5; self-conductance, $w_0$ = 1.0; time step, $\eta_1$ = 0.08). The signal is not fed uniformly to all the cells but weighted in such a way that input to the cells in the center has the highest amplitude. This weighting function is a gaussian window given by: $G = 0.5 \exp\left(-\frac{(j-16)^2}{16} - \frac{(k-16)^2}{16}\right)$, where $j, k = 1, 32$. The neighborhood of connectivity of cells, the values of various parameters ($\lambda, \eta_1, \eta_2$), and initial values of conductances ($w_0$, $w_{n1}$ etc.) are all set as in Sect. 4.2.

Figure 8a–d depicts the model state (Re[$M_{j,k}$]) during the time when stimulation is present and GJ conductances are adapting. A sharp depolarizing impulse begins to rise from the center in Fig. 8a. In Fig. 8b, the initial wave begins to break and spread further. In Fig. 8c, not only is the entire array depolarized but a large repolarizing zone can be seen to be spreading from the center. Repolarization has spread over most of the array in Fig. 8d, with the corners still depolarized. A sizable depolarizing wave now appears at the center. It is interesting to see how an oscillating input applied maximally at the center produces an activation pattern spreading from the center, as though there is a pacemaking zone with maximal intrinsic frequency at the center. Adaptation is continued for 180 time steps, and GJ conductances remain fixed henceforth.

Subsequent evolution of the model is depicted in Fig. 9a–d. Again a depolarizing wave originates at the center in Fig. 9a, and is seen to spread in Fig. 9b. A small repolarizing impulse can already be detected at the center of the array in Fig. 9b. Shortly afterwards (Fig. 9c), the repolarizing wave spreads over the array, which is mostly depolarized; depolarization has not yet reached the corners of the array. In Fig. 9d, repolarization spreads much further.

We may observe that after adaptation the spreading wave is much more precise, which may be attributed to the smoothing effect of adaptation. But the most intriguing development is that repolarizing and depolarizing waves continue to spread as they did when stimulation was present. The only other familiar condition in which such spreading occurs is when a locally maximal intrinsic frequency variation is present. Obviously neither of these conditions is valid here. The reason for the above development is that GJ conductances adapt in such a way that an induced activation sequence is imprinted on, or 'remembered' by, the model. Again, the separation of model evolution into adapting and non-adapting phases is merely to highlight the relative roles played by stimulation and adaptation.

## 6 Discussion

The whole-heart model of Sect. 4.2 can be regarded as two oscillating units (the atrial and ventricular areas) connected by a nonoscillating entity (the AV region). Such an arrangement, compounded with GJ adaptation, automatically introduced a large phase difference between the two oscillating subsystems. Working backwards from the simulations, we are forced to conclude that the AV node might consist, for the most part, of nonoscillating cells, leaving the oscillating junctional cells aside. Even if only oscillating cells are present, still their intrinsic frequency must be distinctly lower than that of the adjacent tissue. The question seems to be not whether there are autorhythmic 'junctional' cells (Guntheroth et al. 1983), but whether there are nonoscillating cells (or cells oscillating at a much lower frequency) on the path connecting atria and ventricles – and our answer is in the affirmative. However, the problem can be solved entirely only when more revealing physiological data are available.

At a more detailed level, the model has several shortcomings. This result is not unexpected since the model is not meant to capture detailed activation patterns of the heart. A

considerable part of AV regional cells showed no significant change in activity; only cells adjacent to the A and V regions seem to oscillate. This problem may perhaps be solved by allowing nodal cells to oscillate, only at a lower rate than the neighboring cells. Another shortcoming is that, contrary to physiology, repolarization of ventricles proceeds in the same direction as depolarization. This might be because of the rapidly conducting Purkinje system in real hearts which is not distinctly represented in our model.

The most important conclusion derivable from these simulations is that cardiac cells are not 'hard-wired' to produce the proper firing sequence – a picture which classic texts on physiology tend to present. The sequence *develops* by GJ adaptation and may itself vary constantly as an expression of the heart's intrinsic adaptability to load variations. This development might possibly take place during the early beats of the developing heart (Kamino 1991). The heart may not exhibit a fully developed conduction sequence when it first began to beat; it is possible that normal out-of-phase AV contractions would follow only after the atria and ventricles have phase-locked by prolonged GJ adaptation.

*Acknowledgements.* The work described here was supported in part by the National Science Foundation under grant ECS-9307632 and in part by ONR Contract N00014-92C-0232. We express our gratitude to Prof. H. Grady Rylander III who graciously agreed to go through the manuscript and give his informed comments.

## References

1. Abbot LF (1990) A network of oscillators. J Phys Math, 23:3835–3859
2. Barry A (1942) The intrinsic pulsation rates of fragments of the embryonic chick heart. J Exp Zool, 91:119–130
3. Chakravarthy SV, Ghosh J (1995) On hebbian-like adaptation in heart muscle: A proposal for 'cardiac memory'. Technical report, Computer and Vision Research Center, The University of Texas at Austin
4. Clapham DE, Shrier A, De Haan RL (1980) Junctional resistance and action potential delay between embryonic cell aggregates. J Gen Physiol, 75:633–654
5. Cohen MA, Grossberg S (1983) Absolute stability of global pattern formation and parallel memory storage by competitive neural networks. IEEE Trans Syst Man Cybern 13:815–826
6. De Haan RL, Hirakow R (1972) Synchronization of pulse rates in isolated myocytes. Exp Cell Res, 70:214–220
7. De Mello WC (1977) Passive electrical properties of the AV node. Pflugers Arch 371:135–139
8. De Mello WC (1982) Intercellular communication in cardiac muscle. Circ Res, 50:2–35
9. Fitzhugh R (1961) Impulses and physiological states in theoretical models of nerve membrane. Biophys J, 1:445–466
10. Goldberger AL, Bhargava V, West BJ, Mandell AJ (1985) Nonlinear dynamics of the heartbeat. II. Subharmonic bifurcations of the cardiac interbeat interval in sinus node disease. Physica D, 17:207–214
11. Guevara MR, Glass L (1982) Phase-locking, period-doubling dynamics and chaos in a periodically driven oscillator: a theory for entrainment of biological oscillators and the generation of cardiac dysrhythmias. J Math Biol 14:1–23
12. Gray CM, Singer W (1989) Stimulus-specific neuronal oscillations in orientation columns of cat visual cortex. Proc Natl Acad Sci USA 86:1698–1702
13. Guntheroth WG, Selzer A, Spodick DH (1983) Atrioventricular rhythm reconsidered. Am J Cardiol, 52:416–417
14. Guyton AC (1981) Textbook of medical physiology. WB Saunders, Philadelphia, chap 14
15. Hebb DO (1949) Organization of behaviour. Wiley, New York
16. Hodgkin AL, Huxley AF (1952) A quantitative description of membrane current and its application to conduction and excitation in nerve. J Physiol (Lond) 117:500–544
17. Jalife J, Michaels DC, Delmar M (1988) Mechanisms of pacemaker synchronization in the sinus node. In: Mazgalev T, Dreyfus LS, Mechelson, EL (esd) Electrophysiology of sinoatrial and atrioventricular nodes. Liss, New York, pp 67–91
18. Kamino K (1991) Optical approaches to ontogeny of electrical activity and related functional organization during early heart development. Physiol Rev 71:53–91
19. Kosko B (1988) Feedback stability and unsupervised learning. In: Proc IEEE Int Conf on Neural Networks, vol. 1. IEEE Press, San Diego, pp 141–152
20. Loewenstein WR (1981) Junctional intercellular communication: the cell-to-cell membrane channel. Physiol Rev 6:829–913
21. Medvinsky AB, Panfilov AV, Pertsov AM (1984) In: Krinsky VI (ed) Self-organization: autowaves and structures far from equilibrium. Springer, Berlin Heidelberg New York
22. Nagumo JS, Arimoto S, Yoshizawa S (1962) An active pulse transmission line simulating nerve axon. Proc IRE 50:2061–2070
23. Noble D (1979) The initiation of heartbeat. Clarendon Press, Oxford
24. Obaid AL, Rose B (1981) Junctional resistance of chironomous cell pairs depends on (nonjunctional) cell potential. Bhiophys J 33:106a
25. Panfilov AV, Winfree AT (1985) Dynamical simulations of twisted scroll rings in three-dimensional excitable media. Physica D 17:323–330
26. Rosenbaum MB, Blanco HH, Elizari MV, Lazzari JO, Davidenko JM (1982) Electrotonic modulation of the T-wave and cardiac memory. Am J Cardiol 50:213–222
27. Rosenbaum MB, Sicouri SJ, Davidenko JM, Elizari MV (1985) Heart rate and electrotonic modulation of the T-wave: a singular relationship. In: Zipes DP, Jalije J (eds) Cardiac electrophysiology and arrhythmias. Grune and Stratton, New York
28. Smith TG, Bauman F (1969) The functional organization within the ommatidium of the lateral eye of *Limulus*. In: Akert K, Waser PG (eds) Progress in Brain Research. Mechanisms of Synaptic Transmission. Elsevier, Amsterdam, pp 314–349
29. Socolar SJ, Politoff L (1971) Uncoupling of cell junctions of a glandular epithelium by depolarizing current. Science 172:492–494
30. Toyoshima H, Burgess MJ (1978) Electrotonic interaction during canine ventricular repolarization. Circ Res 43:348–356
31. van der Pol B (1926) On relaxation oscillations. Phil Mag, Ser 7, 2:978–992
32. van der Pol B, van der Mark J (1928) Phil Mag , 6:763
33. Veenstra RD, De Haan RL (1988) Cardiac gap junction channel activity in embryonic chick ventricle cellls. Am J Physiol 254:H170–H180
34. Wilson FN, MacLeod AG, Barker PS (1931) The T deflection of the electrocardiogram. Trans Assoc Am Physicians 46:29–38